

Electrical conduction processes in ZnO in a wide temperature range 20–500 K

Chien-Chi Lien¹, Chih-Yuan Wu^{2,*}, Zhi-Qing Li³, and Juhn-Jong Lin^{1,4,†}

¹*Institute of Physics, National Chiao Tung University, Hsinchu 30010, Taiwan*

²*Department of Physics, Fu Jen Catholic University, New Taipei City 24205, Taiwan*

³*Tianjin Key Laboratory of Low Dimensional Materials Physics and Preparing Technology, Faculty of Science, Tianjin University, Tianjin 300072, China and*

⁴*Department of Electrophysics, National Chiao Tung University, Hsinchu 30010, Taiwan*

(Dated: October 1, 2018)

We have investigated the electrical conduction processes in as-grown and thermally cycled ZnO single crystal as well as as-grown ZnO polycrystalline films over the wide temperature range 20–500 K. In the case of ZnO single crystal between 110 and 500 K, two types of thermal activation conduction processes are observed. This is explained in terms of the existence of both shallow donors and intermediately deep donors which are consecutively excited to the conduction band as the temperature increases. By measuring the resistivity $\rho(T)$ of a given single crystal after repeated thermal cycling in vacuum, we demonstrate that oxygen vacancies play an important role in governing the shallow donor concentrations but leave the activation energy ($\simeq 27 \pm 2$ meV) largely intact. In the case of polycrystalline films, two types of thermal activation conduction processes are also observed between ~ 150 and 500 K. Below ~ 150 K, we found an additional conduction process due to the nearest-neighbor-hopping conduction mechanism which takes place in the shallow impurity band. As the temperatures further decreases below ~ 80 K, a crossover to the Mott variable-range-hopping conduction process is observed. Taken together with our previous measurements on $\rho(T)$ of ZnO polycrystalline films in the temperature range 2–100 K [Y. L. Huang *et al.*, J. Appl. Phys. **107**, 063715 (2010)], this work establishes a quite complete picture of the overall electrical conduction mechanisms in the ZnO material from liquid-helium temperatures up to 500 K.

PACS numbers: 72.20.My, 71.30.Tm, 73.50.Jt

I. INTRODUCTION

Zinc oxide (ZnO) is a wide band gap semiconductor with a direct energy gap of ≈ 3.4 eV at room temperature. This class of material is usually unintentionally (or, natively) doped with n-type impurities, such as oxygen vacancies, Zn interstitials, and impurity hydrogen atoms. However, the exact doping behavior of different types of unintentional and intentional (e.g., group I or group III) dopants is still under much theoretical and experimental debate.^{1–3}

ZnO has recently attracted intense attention owing to its potential prospects in optoelectronic applications.^{4–6} Compared with the widely studied optical properties, the electrical conduction processes in ZnO materials (single crystals, polycrystalline films, etc.) have not much been investigated over a wide range of temperature.^{7–10} Physically, the measurements on the temperature dependence of resistivity, $\rho(T)$, can provide very useful information on the carrier transport mechanisms as well as the associated impurity levels and their distributions in energy in a given semiconducting material. Recently, Huang *et al.*¹¹ have investigated the electrical conduction processes in a series of oxygen deficient polycrystalline ZnO films (≈ 1 μm thick) in the temperature range 2–100 K. They observed the three-dimensional Mott variable-range-hopping (VRH) conduction process below ~ 100 K. As the temperature further decreased below ~ 25 K, a crossover to the Efros-Shklovskii VRH conduction process was found. These two types of VRH conduction processes in ZnO films have been successfully explained

in a coherent manner. On the other hand, the charge transport properties above 100 K has not been explicitly addressed in that work, due to the lacking of $\rho(T)$ data above 300 K. In this work, we aim at extending the measurements on $\rho(T)$ to temperatures up to 500 K in order to further unravel the overall electrical conduction mechanisms in ZnO, especially at $T \gtrsim 100$ K. We have measured an as-grown ZnO single crystal and re-measured the series of as-grown ZnO polycrystalline films which were first studied in Ref. 11. The as-grown single crystal has been *repeatedly* thermally cycled *in vacuum* and their $\rho(T)$ has been measured during each thermal cycling process. The polycrystalline films had been deposited in different oxygen atmospheres to contain different amounts of oxygen vacancies so that they possessed differing shallow donor concentrations when as prepared. Our new results are reported below.

We would like to emphasize that all the $\rho(T)$ measurements reported in this study have been carried out in a vacuum ($\lesssim 10^{-4}$ torr) and in a “dark” environment without involving any photo-induced carriers. Therefore, complex thermal annealing effects which might result from resistivity measurements performed in, e.g., an air (or an active gas) atmosphere at highly elevated temperatures,¹² can be safely avoided.

This paper is organized as follows. In Sec. II, we briefly discuss our experimental method for sample fabrication and resistance measurements. Our results of the temperature dependence of resistance in the wide temperature interval 20–500 K and their physical interpretations are presented in Sec. III. Section IV contains our conclusion

as well as a summary of the overall electrical conduction mechanisms in the ZnO materials.

II. EXPERIMENTAL METHOD

Our ZnO single crystal ($2.52 \times 1.94 \times 0.45$ mm³) were grown by the hydrothermal method and was obtained from a commercial supplier.¹³ Unfortunately, the detailed growth conditions were unavailable. However, the $\rho(T)$ data do provide us meaningful information on the carrier transport processes in the ZnO material (see below). This as-grown crystal has a room temperature resistivity of $\approx 5.45 \times 10^4$ Ω cm. Our ZnO polycrystalline films were fabricated by the standard rf sputtering deposition method on glass substrates. The starting ZnO target was of 99.99% purity, and the glass substrates were held at 550°C during the deposition process. The films were deposited in varying mixtures of argon and oxygen gases. The $\rho(T)$ of these films had previously been measured and discussed by Huang *et al.*¹¹ for $T \lesssim 100$ K.

In this work, four-probe resistance measurements were carried out using a Keithley Model K-6430 as a current source and a high-impedance (T Ω) Keithley Model K-617 as a voltmeter. The samples were mounted on the sample holder which was situated inside a stainless vacuum can in a JANIS CCS350 closed-cycle refrigerator (10–500 K). The working pressure in the vacuum can was $\lesssim 10^{-4}$ torr throughout all resistivity measurement processes, whether the vacuum can was connected to a diffusion pump (at $T \gtrsim 250$ K) or not (at $T \lesssim 250$ K, see below for further discussion). Moreover, the stainless vacuum can contained no optical windows, and thus our measurements were performed in the dark, i.e., this experiment did not invoke any kind of photo-induced currents. The four-terminal current leads and voltage leads (pogo pins) were attached to the samples with the aid of silver paste. It should be noted that the resistances reported in this work were all measured by scanning the current-voltage (I - V) characteristics at various fixed temperatures between 20 and 500 K. The resistance at a given temperature was determined from the regime around the zero bias voltage, where the I - V curve was linear. In fact, our I - V curves in every sample were linear over a wide range of bias voltage. The inset of Fig. 1 shows the linear I - V characteristics of the as-grown ZnO single crystal at four representative temperatures, as indicated in the caption to Fig. 1.

III. RESULTS AND DISCUSSION

A. ZnO single crystal: thermal activation conduction over 110–500 K

Figure 1 plots the measured resistivity as a function of reciprocal temperature for the as-grown single crystal between 110 and 500 K. (The resistance below ~ 110 K be-

came too large to be accurately measured.) Two distinct slopes are explicitly seen in the two different temperature regimes of ~ 110 –220 K (straight dotted line) and ~ 290 –500 K (straight dashed line), respectively. Such Arrhenius-type behavior immediately suggests that the responsible charge transport arises from the thermal activation conduction processes. Indeed, we found that our measured $\rho(T)$ data can be quantitatively described by the equation

$$\rho(T)^{-1} = \rho_1^{-1} e^{-E_1/k_B T} + \rho_2^{-1} e^{-E_2/k_B T}, \quad (1)$$

where ρ_1 and ρ_2 are temperature insensitive resistivity prefactors, and E_1 and E_2 are the relevant activation energies associated with the two kinds of thermal activation conduction processes. k_B is the Boltzmann constant. In Fig. 1, the solid curve is a least-square fit to Eq. (1). It clearly manifests that Eq. (1) can well describe the experimental result. Our fitted values of ρ_1 , E_1 , ρ_2 , and E_2 are listed in Table I. This observation illustrates that there exist in the as-grown single crystal a group of shallow donors with an activation energy of $E_2 \approx 29$ meV and a group of intermediately deep donors with an activation energy of $E_1 \approx 330$ meV. (In this work, we shall maintain the convention $E_1 > E_2$.) At the sufficiently high measurement temperatures of $T \gtrsim 290$ K, both the shallow and the intermediately deep donors are excited to the conduction band and are responsible for the electrical transport. However, the exponential temperature dependence of ρ is mainly governed by the number of those intermediately deep donors which are being excited to the conduction band (the so-called E_1 -conduction channel). As T reduces below ~ 220 K, the intermediately deep donors become essentially intact while the shallow donors can still be readily excited to the conduction band. The T dependence of ρ is thus largely determined by the number of those shallow donors being excited to the conduction band (the so-called E_2 -conduction channel). In short, Eq. (1) represents the “band conduction” processes.

It should be noted that our extracted E_1 and E_2 values are in good accord with the corresponding activation energies previously obtained by Look⁶ (~ 340 meV), Wenckstern *et al.*¹⁴ (~ 34 –37 and ~ 300 –370 meV), and Schifano *et al.*¹⁵ (~ 30 , ~ 50 , and ~ 290 meV) in various ZnO single crystals and in different temperature intervals. Recently, in a series of single-crystalline ZnO nanowires, Chiu *et al.*¹⁶ (Tsai *et al.*¹⁷) have also reported an E_2 activation energy of ~ 30 –40 (~ 25) meV. In other words, we may conclude that different ZnO single crystals grown by differing methods and under differing conditions possess essentially similar types of shallow and intermediately deep donor levels. (Obviously, the donor concentrations would vary from experiment to experiment.)

In Fig. 2, we plot our measured resistivities as a function of reciprocal temperature for the as-grown and then repeatedly thermally cycled single crystal. The closed squares (taken from Fig. 1), open squares, closed circles, and open circles represent the as-grown, first-cycled, second-cycled, and third-cycled samples, respectively. In

TABLE I. Relevant parameters of as-grown and thermally cycled ZnO single crystal. ρ_1 , E_1 , ρ_2 , and E_2 are defined in Eq. (1).

single crystal	$\rho(300\text{ K})$ ($\Omega\text{ cm}$)	ρ_1 ($\Omega\text{ cm}$)	E_1 (meV)	ρ_2 ($\Omega\text{ cm}$)	E_2 (meV)
as-grown	5.45×10^4	0.144	334	1.47×10^5	29.2
first-cycled	4.56×10^4	0.154	330	2.50×10^4	28.1
second-cycled	2.70×10^4	0.145	332	1.72×10^4	24.7
third-cycled	2.01×10^4	0.125	337	1.02×10^4	26.4

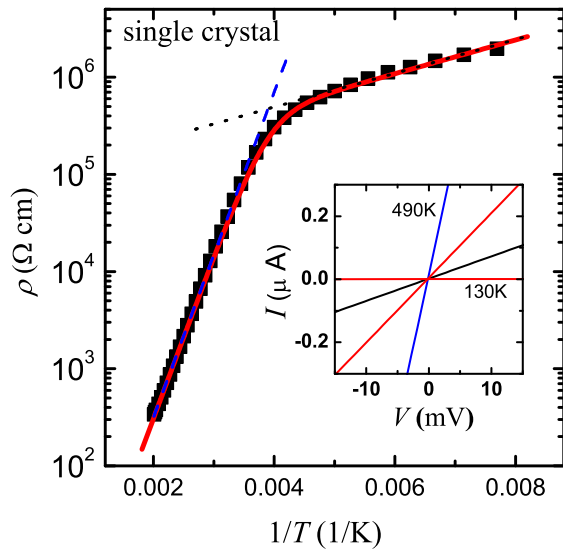


FIG. 1. (color online) Logarithm of resistivity as a function of reciprocal temperature for as-grown ZnO single crystal between 110 and 500 K. The symbols are the experimental data and the solid curve is a least-squares fit to Eq. (1). The straight dashed and dotted lines are guides to the eye. Inset: Current-voltage curves at four temperatures of 490, 410, 370, and 130 K. Notice that the I - V characteristics are linear, i.e., ohmic.

practice, our $\rho(T)$ data for every sample were measured from 500 K down. The sample was placed in the dark vacuum can and first heated to 500 K. The T dependence of ρ was then measured with progressive lowering of temperature. During the data acquisition process from 500 K down to 250 K, the dark vacuum can was connected to a diffusion pump for continuous pumping. The diffusion pump was disconnected when the temperature reached 250 K.¹⁸ Such a measurement process (which lasted for ~ 270 min between 250 and 500 K) had effectively served as a “thermal annealing” (in vacuum) process. Therefore, the oxygen contain in the sample was reduced from that in the previous run. In other words, the amount of oxygen vacancies increased, leading to a decrease in the sample resistivity. We have repeated the $\rho(T)$ measurements in the temperature interval 110–500 K for four times, and denoted the sample by as-grown, first-cycled, second-cycled, and third-cycled samples, as mentioned.

Inspection of Fig. 2 indicates that, in the temperature interval ~ 330 –500 K, the $\rho(T)$ data collapse closely onto

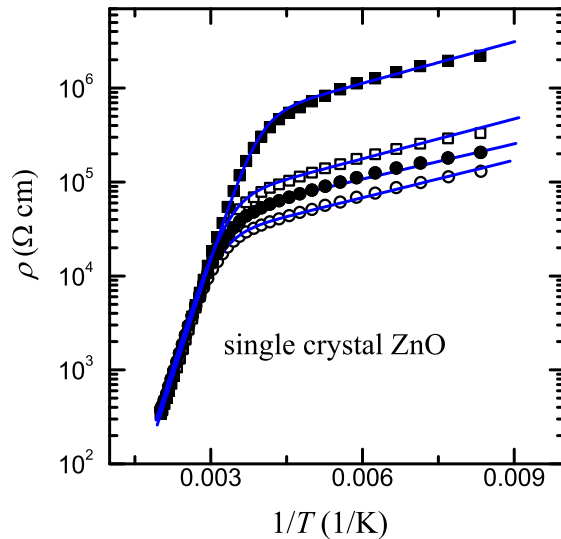


FIG. 2. (color online) Logarithm of resistivity as a function of reciprocal temperature for the as-grown (closed squares, taken from Fig. 1), first-cycled (open squares), second-cycled (closed circles), and third-cycled (open circles) ZnO single crystal. The solid curves are least-squares fits to Eq. (1), see text.

a straight line. On the other hand, below ~ 330 K, the measured $\rho(T)$ data systematically decrease after each repeated thermal cycling. Quantitatively, the resistivity ratios of the as-grown sample to the third-cycled sample are $\simeq 1.0$ at 460 K, $\simeq 2.7$ at 300 K, and $\simeq 11$ at 220 K. This variation in resistivity ratio suggests that the rich amount of the intermediately deep donors¹⁹ and their associated activation energies, i.e., the E_1 values, are barely affected by our measuring and/or thermal cycling process. This is expected, since the activation energies associated with these donor levels are comparatively large while our thermal cycling temperature is relatively low.

What is more interesting is the T behavior of ρ between 110 and 220 K. While the ρ value at a given T decreases with repeated thermal cycling as mentioned, the *temperature dependence* of ρ maintains essentially *unchanged*. Numerically, our least-squares fitted slopes, i.e., the E_2 values, in this temperature interval vary only by $\sim 10\%$, see Table I. This quantitative result is meaningful. It strongly implies that the amount of oxygen vacancies, namely, the shallow donor concentration, in the sample is increased after each repeated thermal cycling. Never-

theless, the thermal activation energy, namely, the shallow donor level below the conduction band minimum, remains essentially unchanged. (See Ref. 20 for a brief discussion on the thermal-cycling-induced weak dispersion of the shallow donor energy levels.) This observation is strongly supportive of the important roles of oxygen vacancies as the shallow donors in ZnO. On the theoretical side, based on the formation energy consideration, it has recently been argued that oxygen vacancies would form negative-U centers, rather than shallow donors, in the ZnO material.^{21–24} This theoretical prediction is not supported by the present result, Fig. 2. This puzzling issue requires further clarification.

B. ZnO polycrystalline films

1. Thermal activation conduction and nearest-neighbor-hopping conduction: 90–500 K

Figure 3 shows the variation in the logarithm of resistivity with reciprocal temperature for four ZnO polycrystalline films between 90 and 500 K, as indicated. In sharp contrast to the case of single crystal (Fig. 2), Fig. 3 clearly reveals that ρ smoothly increases with decreasing temperature. That is, there does not exist a visible straight regime in any temperature interval in the $\log\rho$ –($1/T$) plot from 500 down to 90 K. Quantitatively, we found that these results can not be described by Eq. (1). Instead, they can be described by the following equation

$$\rho(T)^{-1} = \rho_1^{-1} e^{-E_1/k_B T} + \rho_2^{-1} e^{-E_2/k_B T} + \rho_3^{-1} e^{-E_3/k_B T}, \quad (2)$$

where ρ_1 , E_1 , ρ_2 , and E_2 have the similar meaning as defined in Eq. (1). The third term on the right hand side represents a new, additional electrical conduction channel which is characterized by a temperature insensitive resistivity prefactor ρ_3 and a thermal activation energy E_3 . (In the following discussion, we shall maintain the convention $E_1 > E_2 > E_3$.)

Our fitted results with Eq. (2) are plotted as the solid curves in Fig. 3 and the values of the adjustable parameters are listed in Table II. We obtain the thermal activation energies $E_1 \approx 113$ –135 meV, $E_2 \approx 26$ –39 meV, and $E_3 \approx 2.3$ –5.7 meV. The three types of conduction processes dominate the T dependence of ρ in the temperature intervals of ~ 400 –500 K (the E_1 -conduction channel), ~ 150 –400 K (the E_2 -conduction channel), and ~ 90 –150 K (the E_3 -conduction channel). Physically, the E_1 - and the E_2 -conduction processes are just those described in the above subsection. However, the E_1 activation energy is markedly reduced from ≈ 330 meV for single crystal to $\approx 125 \pm 10$ meV for polycrystalline films (see further discussion below). The additional E_3 -conduction channel can be ascribed to the nearest-neighbor-hopping (NNH) conduction mechanism which takes place in the shallow “impurity band.” That is, as the temperature decreases below ~ 150 K, even the shallow donors (not mentioning

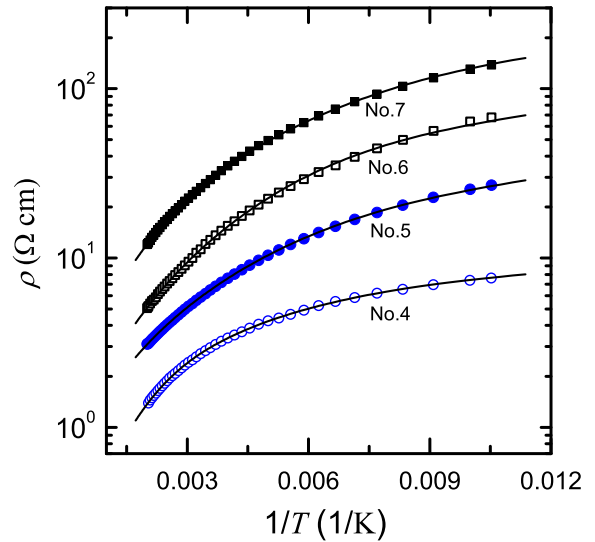


FIG. 3. Logarithm of resistivity as a function of reciprocal temperature for four ZnO polycrystalline films between 90 and 500 K, as indicated. The symbols are the experimental data and the solid curves are least-squares fits to Eq. (2).

the intermediately deep donors) can no longer be effectively excited to the conduction band. The charge transport is then largely governed by those electrons which hop from an occupied state (which lies below the Fermi energy) to an unoccupied nearest-neighbor state (which lies above the Fermi energy) in the impurity band. Such a hopping process is phonon assisted and requires a small amount of energy, i.e., the E_3 thermal activation energy. It should be noted that a shallow impurity band can form in the oxygen deficient ZnO polycrystalline films but not in the ZnO single crystal, because the former samples contain far higher amounts of oxygen vacancies. A large amount of oxygen vacancies causes a notable dispersion of the donor levels or ionization energies, and thus forming an impurity band.²⁵ Due to the slight self-compensation characteristic of unintentionally doped ZnO,^{16,26} the impurity band is partially filled, making the NNH conduction process possible. Based on this picture, the E_3 value should decrease with increasing oxygen vacancies, because there would be more randomly distributed donor levels per unit energy per unit volume. Indeed, inspection of Table II reveals that our extracted E_3 value (on average) decreases with the decreasing O_2 flux applied during the fabrication process.

In contrast, in the case of single crystal, the shallow donor concentration is sufficiently low and thus, on average, the donor impurities should lie sufficiently far apart in space and in energy. Therefore, the NNH conduction process can only play a negligible role, as compared to the E_2 -conduction process, even at temperatures down to 110 K. Inspection of Tables I and II indicates that the $\rho(300\text{ K})$ values of our polycrystalline films are more than

TABLE II. Values of relevant parameters for six oxygen deficient ZnO polycrystalline films. ρ_i ($i=1, 2, 3$) and E_i are defined in Eq. (2). Notice that these samples are taken from Ref. 11 and remeasured from 500 K down. As a result of thermal cycling/annealing in this study (see text), the resistivity values are lowered by $\sim 20\%$ from those corresponding values originally reported in Ref. 11.

Film No.	O ₂ flux (SCCM)	$\rho(300\text{ K})$ ($\Omega\text{ cm}$)	ρ_1 ($\Omega\text{ cm}$)	E_1 (meV)	ρ_2 ($\Omega\text{ cm}$)	E_2 (meV)	ρ_3 ($\Omega\text{ cm}$)	E_3 (meV)
2	0.02	1.66	0.079	120	1.89	35.5	2.63	2.3
3	0.10	2.72	0.407	113	0.758	39.2	5.00	3.1
4	0.15	2.01	0.189	135	1.30	37.5	5.88	2.8
5	0.25	5.89	0.420	135	2.70	26.3	370	5.7
6	0.50	11.3	0.588	129	4.79	27.0	333	5.6
7	0.80	26.0	2.04	121	9.09	37.7	100	4.3

3 orders of magnitude lower than that in the single crystal. Such huge differences in resistivity provide a direct indication of the presence of far more numerous amounts of oxygen vacancies in polycrystalline films than in single crystal. (The shallow donor concentrations in the polycrystalline films will be estimated in the subsection IIIB.3.)

Our extracted E_2 values of ≈ 26 – 39 meV for the shallow donors are in consistency with those previously reported for the ZnO materials.^{16,26} Our extracted E_1 values of $\approx 125 \pm 10$ meV are in line with that (≈ 110 meV) deduced by Tampo *et al.*²⁷ in ZnO films grown by radical source molecular-beam epitaxy. However, these E_1 values are significantly lower than that (≈ 330 meV) found in the single crystal discussed in the above subsection. The reason why requires further investigation. One plausible explanation would be that, as compared with the single crystal, there are additional impurity levels which were unintentionally introduced during the growth of the polycrystalline films. On the other hand, since the E_2 -conduction channel dominates the electrical-transport behavior up to ~ 400 K in our films, electrical measurements up to T sufficiently higher than 500 K would be highly desirable for an unambiguous determination of the values of the E_1 activation energy and the associated charge conduction process.²⁸

2. Three-dimensional Mott variable-range-hopping conduction: 20–80 K

As mentioned, our ZnO polycrystalline films had been measured previously in Ref. 11. In this work, we have extended the $\rho(T)$ measurements on these films up to 500 K. Notice that these measurements have led to thermal cycling/annealing effect (in vacuum) on these films. As a result, their $\rho(T)$ values are changed from the corresponding values originally reported in Ref. 11. In particular, the $\rho(T)$ values are largely reduced in those films grown under high oxygen atmospheres. For instance, the $\rho(300\text{ K})$ value decreased from 206 to 26 $\Omega\text{ cm}$ in the film No. 7. Nevertheless, we would expect the charge conduction mechanisms, i.e., the Mott and the Efros-Shklovskii

VRH conduction processes previously observed below ~ 90 K as mentioned in the Introduction, to be robust. This assertion is examined in the following.

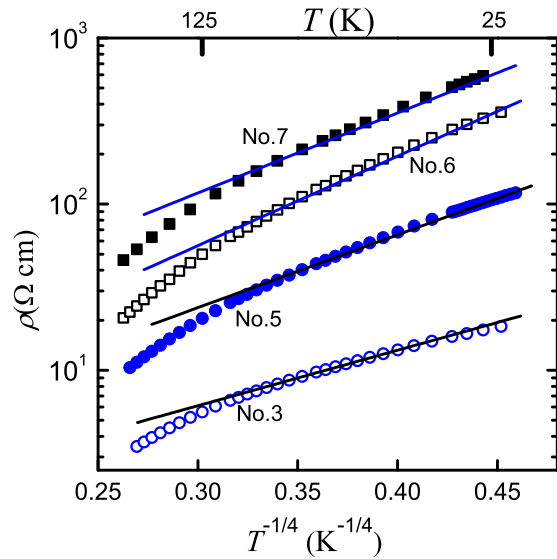


FIG. 4. (color online) Logarithm of resistivity as a function of $T^{-1/4}$ for four ZnO polycrystalline films, as indicated. The symbols are the experimental data and the straight solid lines are least-squares fits to Eq. (3).

Figure 4 plots the variation of $\log \rho$ with $T^{-1/4}$ for four representative ZnO films, as indicated. The symbols are the experimental data and the straight solid lines are the least-squares fits to the Eq. (3) given below. Clearly, in every sample, there exists a linear regime from ~ 80 K down to ~ 25 K. This observation suggests that, in this T interval, the dominate electrical conduction process is due to the Mott VRH conduction mechanism in three dimensions:²⁵

$$\rho_M(T) = \rho_{M0} e^{(T_M/T)^{1/4}}, \quad (3)$$

where ρ_{M0} is a temperature insensitive resistivity parameter, and $T_M = 18/[k_B N(E_F) \xi^3]$ is a characteristic temperature. $N(E_F)$ is the electronic density

TABLE III. Values of relevant parameters for six oxygen deficient ZnO polycrystalline films. ρ_{M_0} and T_M are defined in Eq. (3). $N(E_F)$ is the electronic density of states at the Fermi energy, $\bar{R}_{\text{hop,Mott}}$ is the average hopping distance, ξ is the Bohr radius of the shallow donors, and $\bar{W}_{\text{hop,Mott}}$ is the average hopping energy. The values of $\bar{W}_{\text{hop,Mott}}$ were calculated for a representative temperature of 40 K.

Film No.	ρ_{M_0} (Ω cm)	T_M (K)	$N(E_F)$ ($\text{J}^{-1} \text{ m}^{-3}$)	$\frac{\bar{R}_{\text{hop,Mott}}}{\xi}$	$\bar{W}_{\text{hop,Mott}}$ (meV)
2	1.36	65	2.5×10^{48}	$1.07/T^{1/4}$	0.98
3	0.61	3510	4.6×10^{46}	$2.89/T^{1/4}$	2.64
4	1.41	854	1.9×10^{47}	$2.03/T^{1/4}$	1.85
5	1.15	10400	1.6×10^{46}	$3.79/T^{1/4}$	3.35
6	1.36	23600	6.9×10^{45}	$4.65/T^{1/4}$	4.14
7	4.18	15200	1.1×10^{46}	$4.16/T^{1/4}$	3.68

of states at the Fermi level, and ξ is the localization length of the relevant electronic wave function. The average hopping distance and the average hopping energy of the conduction electrons are, respectively, given by $\bar{R}_{\text{hop,Mott}} = (3\xi/8)(T_M/T)^{1/4}$ and $\bar{W}_{\text{hop,Mott}} = (k_B T/4)(T_M/T)^{1/4}$.²⁹ Our extracted values of T_M , and then calculated values of $N(E_F)$, $\bar{R}_{\text{hop,Mott}}$, and $\bar{W}_{\text{hop,Mott}}$ are listed in Table III. In order to calculate these three quantities, we have used $\xi \approx 2$ nm, the Bohr radius of the shallow donors in ZnO.² Our fitted $\bar{R}_{\text{hop,Mott}}$ values are significantly smaller than our film thickness ($\approx 1 \mu\text{m}$). Also, the criterion $\bar{R}_{\text{hop,Mott}}/\xi > 1$ for Eq. (3) to be valid is satisfied in the films Nos. 3 and 5–7. On the other hand, this criterion is not satisfied for the films Nos. 2 and 4, because these two films are not resistive enough to lie sufficiently deep on the insulating side of the metal-insulator transition.¹¹ Furthermore, our extracted values of $\bar{W}_{\text{hop,Mott}}(40 \text{ K}) \approx 1\text{--}4$ meV are somewhat smaller than the corresponding values reported in Ref. 11. This small decrease in $\bar{W}_{\text{hop,Mott}}$ by $\sim 35\%$ from that in Ref. 11 can be readily understood as arising from the increased shallow donor concentrations in these films as a result of thermal cycling/annealing. Obviously, on average, a higher donor concentration will lead to a lower thermal activation energy involved in the VRH conduction process.

Our observation of the Mott VRH conduction in the T interval $\sim 20\text{--}80$ K in this work demonstrates that this carrier transport process in the ZnO material is generic and robust, while the values of the relevant parameters may differ somewhat from run to run, because the amounts of donor concentration could have varied. At even lower measurement temperatures ($\lesssim 20$ K), a crossover from the Mott VRH conduction process to the Efros-Shklovskii VRH conduction process³⁰ should be expected, as has previously been reported in Ref. 11. Unfortunately, the base temperature of our closed-cycle refrigerator does not allow $\rho(T)$ measurements down to sufficiently low T to illustrate this latter VRH conduction mechanism in the present work.

3. Estimate of shallow donor concentration

While the shallow donor concentration, n_D , in the ZnO material is a very important quantity, it is difficult to measure directly. However, we may estimate this quantity from the extracted ρ_2 value which characterizes the E_2 -conduction channel in Eqs. (1) and (2). At sufficiently high temperatures (in practice, above a few hundreds K), the shallow donors should have essentially all been ionized. These excited electrons would move in the conduction band and be in response to an externally applied electric field. The resulted electrical conductivity from this E_2 -conduction channel can approximately be expressed by $\rho_2^{-1} = (n_D e^2 \tau_e)/m^* = n_D e \mu_e$, where τ_e is the electron elastic mean free time, m^* is the effective electron mass, and μ_e is the electron mobility. Typically, the value of μ_e in ZnO at T above a few hundreds K can be extrapolated to a magnitude of $\sim 10 \text{ cm}^2/\text{Vs}$.⁴ In the case of our as-grown single crystal, Table I lists a value $\rho_2 \sim 1 \times 10^4 \Omega \text{ cm}$. Then, we may estimate $n_D = (\rho_2 e \mu_e)^{-1} \sim 10^{14} \text{ cm}^{-3}$. In the case of our polycrystalline films, Table II lists a value $\rho_2 \sim 1 \Omega \text{ cm}$. Then, we may estimate $n_D = (\rho_2 e \mu_e)^{-1} \sim 10^{18} \text{ cm}^{-3}$. These inferred shallow donor concentrations in the single crystal and in the polycrystalline films, respectively, are in good accord with the accepted corresponding values reported in the literature.^{4,26} This degree of agreement provides a self-consistency check of our data analyses and the interpretation of the charge transport processes in ZnO in this section.

IV. CONCLUSION AND SUMMARY

We have investigated the electrical conduction properties of ZnO single crystal and polycrystalline films in the wide temperature range $20\text{--}500$ K. In the case of single crystal, we found that two types of thermal activation conduction processes dominate the carrier transport at $T \gtrsim 110$ K. As a result, a group of shallow donors and a group of intermediately deep donors, together with their individual ionization energies, have been inferred. In par-

ticular, we observed that the shallow donor concentration is markedly affected by thermal cycling in vacuum, strongly suggesting the important role of oxygen vacancies as shallow donors in the ZnO material. In the case of oxygen deficient polycrystalline films, additional conduction processes due to the nearest-neighbor-hopping conduction and the Mott variable-range-hopping conduction mechanisms are observed. These two additional conduction processes originate from the existence of far more numerous amounts of shallow donors (oxygen vacancies) in polycrystal films, which led to the formation of a partially filled impurity band. Taken together with our previous work (Ref. 11), this present study provides a fairly complete picture of the overall electrical conduction processes in the ZnO materials.

A summary of the overall electrical conduction processes in the ZnO materials: We would like to give a brief summary of the rich electrical conduction processes in the intensively studied, scientifically and technologically alluring ZnO materials. As the temperature progressively increases from liquid-hilum temperatures up to 500 K, one expects to see, one process by one process, (1) the Efros-Shklovskii variable-range hopping conduction, (2) the Mott variable-range hopping conduction, (3) the nearest-neighbor-hopping conduction, (4) the thermal activation conduction from the shallow donor levels,

and finally (5) the thermal activation conduction from the intermediately deep donors levels. The conduction processes (1)–(3) take place in the shallow donor impurity band, while the conduction processes (4) and (5) take place in the conduction band. These conduction mechanisms are generic and robust in unintentionally doped n-type ZnO materials which lie on the insulating side of the metal-insulator transition.³¹ However, the temperature interval within which each conduction mechanism is found and the extracted value of the associated parameter may vary more or less from experiment to experiment. Such variations can readily arise from the fact that different experiments usually involve differing amounts of donors and differing donor level distributions in the samples.

ACKNOWLEDGMENTS

The authors are grateful to S. P. Chiu for experimental assistance and valuable discussion. This work was supported by the Taiwan National Science Council through Grant No. NSC 99-2120-M-009-001 and the MOE ATU Program (J.J.L.), and by the Key Project of Chinese Ministry of Education through Grant No. 109042 and NSF of Tianjin City through Grant No. 10JCYBJC02400 (Z.Q.L.).

-
- * Electronic address: 016287@mail.fju.edu.tw
† Electronic address: jjlin@mail.nctu.edu.tw
- ¹ A. Janotti and C. G. Van de Walle, Rep. Prog. Phys. **72**, 126501 (2009).
 - ² M. D. McCluskey and S. J. Jokela, J. Appl. Phys. **106**, 071101 (2009).
 - ³ Ü. Özgür, Y. I. Alivov, C. Liu, A. Teke, M. A. Reshchikov, S. Doğan, V. Avrutin, S.-J. Cho, and H. Morkoc, J. Appl. Phys. **98**, 041301 (2005).
 - ⁴ K. Ellmer, in *Transparent Conductive Zinc Oxide*, edited by K. Ellmer, A. Klein, and B. Rech (Springer, New York, 2008), Chap. 2.
 - ⁵ Z. Q. Li, D. X. Zhang, and J. J. Lin, J. Appl. Phys. **99**, 124906 (2006).
 - ⁶ D. C. Look, Mater. Sci. Eng. B **80**, 383 (2001).
 - ⁷ R. Kumar and N. Khare, Thin Solid Films **516**, 1302 (2008).
 - ⁸ A. Tiwari, C. Jin, J. Narayan, and M. Park, J. Appl. Phys. **96**, 3827 (2004).
 - ⁹ S. P. Heluani, G. Braunstein, M. Villafuerte, G. Simonelli, and S. Duhalde, Thin Solid Films **515**, 2379 (2006).
 - ¹⁰ T. Tsurumi, S. Nishizawa, N. Ohashi, and T. Ohgaki, Jpn. J. Appl. Phys., Part 1 **38**, 3682 (1999).
 - ¹¹ Y. L. Huang, S. P. Chiu, Z. X. Zhu, Z. Q. Li, and J. J. Lin, J. Appl. Phys. **107**, 063715 (2010).
 - ¹² Y. Zhang, G. Du, X. Yang, B. Zhao, Y. Ma, T. Yang, H. C. Ong, D. Liu, and S. Yang, Semicond. Sci. Technol. **19**, 755 (2004).
 - ¹³ MTI Corporation, 860 South 19th Street, Richmond, CA 94804, USA.
 - ¹⁴ H. von Wenckstern, M. Brandt, H. Schmidt, G. Biehne, R. Pickenhain, H. Hochmuth, M. Lorenz, and M. Grundmann, Appl. Phys. A **88**, 135 (2007).
 - ¹⁵ R. Schifano, E. V. Monakhov, B. G. Svensson, W. Mtangi, P. Janse van Rensburg, and F. D. Aurret, Physica B **404**, 4344 (2009).
 - ¹⁶ S. P. Chiu, Y. H. Lin, and J. J. Lin, Nanotechnology **20**, 015203 (2009).
 - ¹⁷ L. T. Tsai, S. P. Chiu, J. G. Lu, and J. J. Lin, Nanotechnology **21**, 145202 (2010).
 - ¹⁸ Well below room temperatures, the closed-cycle refrigerator served as a cryopump. The diffusion pump was therefore disconnected to prevent a backflow of its oil vapor into the refrigerator.
 - ¹⁹ The intermediately deep donor concentration should be much higher than the shallow donor concentration. This can be seen from the fact that, once T is sufficiently high and the intermediately deep donors are excited, the E_1 -conduction channel dominates the sample conductance. Notice that in Table I the ρ_1 values are 5 to 6 orders of magnitude lower than the corresponding ρ_2 values. An estimate of the shallow donor concentration is given in subsection IIIB.3.
 - ²⁰ Strictly speaking, the E_2 values are slightly reduced from ≈ 29 to ≈ 25 – 26 meV after repeated thermal cycling. This can be ascribed to a slight increase in the donor concentration and thus an associated weak dispersion of the shallow impurity levels.
 - ²¹ A. Janotti and C. G. Van de Walle, Appl. Phys. Lett. **87**, 122102 (2005).

- ²² L. S. Vlasenko and G. D. Watkins, Phys. Rev. B **71**, 125210 (2005).
- ²³ S. B. Zhang, S.-H. Wei, and A. Zunger, Phys. Rev. B **63**, 075205 (2001).
- ²⁴ S. Lany and A. Zunger, Phys. Rev. B **72**, 035215 (2005).
- ²⁵ N. F. Mott and E. A. Davis, *Electronic Processes in Non-Crystalline Materials*, 2nd ed. (Clarendon, Oxford, 1979).
- ²⁶ D. C. Look, C. Coskun, B. Claflin, and G. C. Farlow, Physica B **340–342**, 32 (2003).
- ²⁷ H. Tampo, A. Yamada, P. Fons, H. Shibata, K. Matsubara, K. Iwata, S. Niki, K. Nakahara, and H. Takasu, Appl. Phys. Lett. **84**, 4412 (2004).
- ²⁸ In case the grain boundary in a polycrystalline semiconductor film forms a depletion region, the thermionic emission effect on the electrical conduction might need to be taken into consideration. See, for example, Refs. 9 and 10. In this study, our films are single-phased and possess a good *c*-axis texture (Ref. 11), and thus the grain boundary effect does not play a notable role.
- ²⁹ V. F. Gantmakher, *Electrons and Disorder in Solids*, (Clarendon, Oxford, 2005).
- ³⁰ B. I. Shklovskii and A. L. Efros, *Electronic Properties of Doped Semiconductors* (Springer, New York, 1984).
- ³¹ If a sample lies sufficiently close to the metal-insulator transition, the “split-impurity-band” conduction process may take place, as has recently been observed in relatively heavily and natively doped, single-crystalline ZnO nanowires (Refs. 16 and 17). In this case, the shallow impurity band splits into a lower subband and an upper subband as a consequence of the presence of excessive randomness and strong Coulomb interactions, see Refs. 25 and 30.